

Xenon in Rigid Oxide Frameworks: Structure, Bonding and Explosive Properties of Layered Perovskite $K_4Xe_3O_{12}$

Sergey N. Britvin,^{*,†} Sergei A. Kashtanov,[‡] Sergey V. Krivovichev,[†] and Nikita V. Chukanov[‡]

[†]Department of Crystallography, Saint-Petersburg State University, Universitetskaya Nab. 7/9, 199034 St. Petersburg, Russia

[‡]Institute of Problems of Chemical Physics, Russian Academy of Sciences, 142432 Chernogolovka, Russia

Supporting Information

ABSTRACT: The tendency of high-valence xenon to form consolidated oxide structures is herein supported by the study of $K_4Xe_3O_{12}$, the first example of a layered xenon perovskite. Xenon seems to be the only nontransition element that can adopt single-cation oxide perovskite frameworks. At the same time, peculiarities of electronic structure of xenon impose specific features on the bonding within a perovskite structure. Weak supramolecular interactions known as aerogen bonds are the linkers that maintain structural integrity of perovskite slabs in $K_4Xe_3O_{12}$. The occurrence of aerogen bonding can provide an insight into the explosive properties of $K_4Xe_3O_{12}$: the weakness of supramolecular interactions allows consideration of them as possible trigger bonds responsible for the detonation sensitivity of layered xenon perovskite.

Current studies in the chemistry of xenon are focused on its supramolecular, covalent, and coordination interactions in low-valence states,¹ with a much lesser number of publications related to ionic compounds.² The latter field of Xe chemistry has been renewed by the synthesis of perovskites with the framework-forming xenon.³ In the present study, we demonstrate that incorporation of xenon into rigid oxide frameworks is not a chemical curiosity but apparent tendency for this noble gas in higher oxidation states. We report on unusual example of a layered xenon oxide with a hexagonal perovskite structure where perovskite-type units are composed entirely of xenon–oxygen octahedra.

The history of this compound, the yellow salt $K_4Xe_3O_{12}$, goes back to the pioneering works in xenon chemistry.⁴ Its composition was found to correspond to the formula $K_4XeO_6 \cdot 2XeO_3$ meaning that the compound contains both octa- and hexavalent xenon.^{4c} However, its structural nature was not revealed at the time. The latter could in part be related to explosive properties of $K_4Xe_3O_{12}$; it is highly shock-sensitive and violently explodes in the dry state.⁴ We succeeded in the growth of $K_4Xe_3O_{12}$ crystals suitable for contemporary single-crystal studies (Figure 1)^{5,6} and found that it exhibits a spectacular layered perovskite structure (Figure 2). $K_4Xe_3O_{12}$ belongs to the family of 12-layer cation-deficient hexagonal perovskites.⁷ The archetype compound of this series is $La_4Ti_3O_{12}$,⁸ and the generalized formula of the members can be expressed as $A_4B_3\Box O_{12}$, where A is a large cation in a cubooctahedral coordination, B the transition metal,^{7,9} and the box \Box denotes octahedral vacancy.⁷ The basic structural unit is



Figure 1. Aggregate of $K_4Xe_3O_{12}$ platelets.

a rigid three-layer slab composed of corner-sharing metal–oxygen octahedra. The slabs are interleaved with the layers of octahedral vacancies to form 12-layer hexagonal perovskite stacking (Figure 2). The fascinating feature of $K_4Xe_3O_{12}$ is that perovskite slabs in its structure are composed entirely of XeO_6 octahedra. The inner layer of each slab consists of corner-sharing XeO_6 (perxenate) octahedra (Figure 2, Table 1). This Xe(VIII) layer is sandwiched between the outer Xe(VI) layers, which are, in a strict chemical sense, composed of neutral XeO_3 molecules (Figure 2b). The apex of each XeO_3 pyramid is directed toward inner layer forming severely distorted $[O_3\cdots XeO_3]$ octahedron (Figure 2c) where Xe(VI) is bonded to the three oxygens of XeO_3 molecule [$d(Xe–O) = 1.774 \text{ \AA}$]. Of particular interest are the three other linkages with $d(Xe–O) = 2.475 \text{ \AA}$ (Table 1), which is much less than the sum of the van der Waals radii of xenon and oxygen (3.80 \AA) but considerably exceeds the sum of their covalent radii (2.03 \AA).¹⁰ The results of computations using the methods of quantum theory of atoms-in-molecules (QTAIM)^{11–16} reveal the existence of Xe–O bond paths coincident with the long Xe–O linkages. The QTAIM properties of bond critical points (BCPs) corroborate with the properties of recently defined type of supramolecular interactions: σ -hole aerogen bonding (Table 1).¹⁷

Table 1 summarizes xenon–oxygen bond properties of $K_4Xe_3O_{12}$ and neat XeO_3 (the latter is a prototype compound featuring aerogen bonds). There is expected positive correlation between the bond length and its strength: aerogen interactions in $K_4Xe_3O_{12}$ are considerably weaker than covalent bonds between xenon and oxygen as it is confirmed by the respective values of electron density (ρ_b) at the BCPs. The positive sign of

Received: August 29, 2016

Published: October 12, 2016

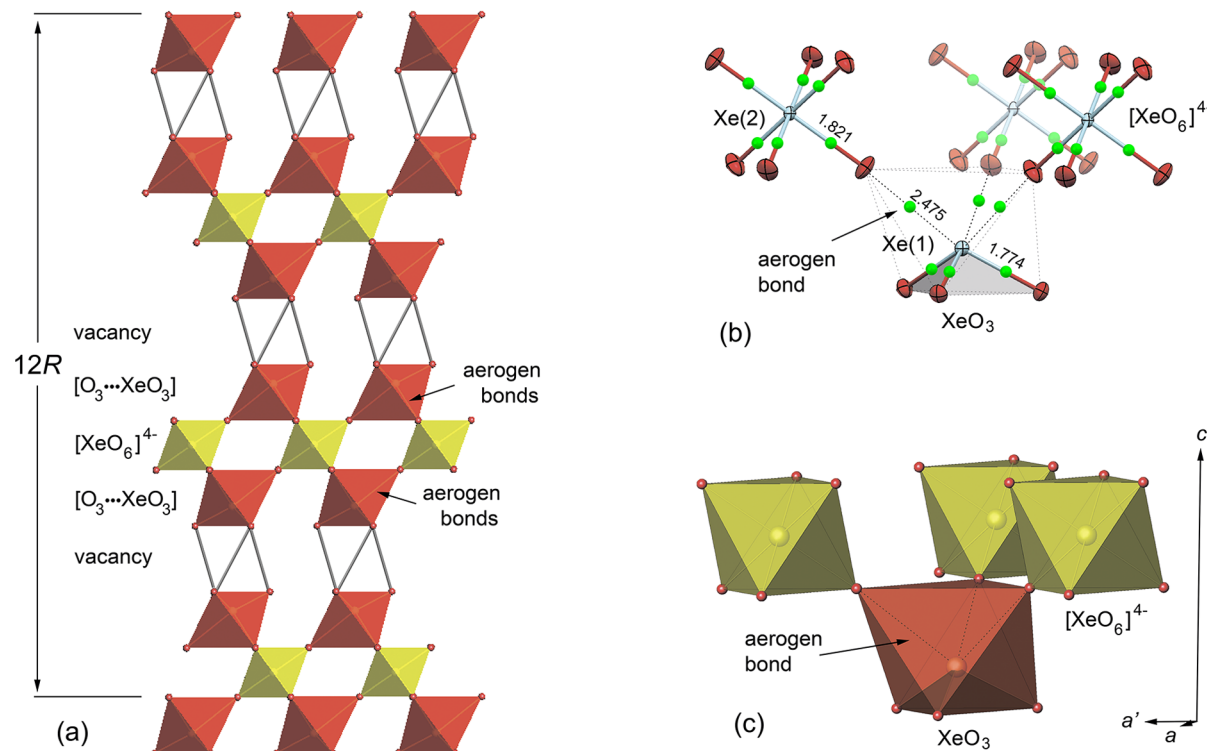


Figure 2. Hexagonal perovskite structure of $\text{K}_4\text{Xe}_3\text{O}_{12}$. (a) Projection along the *c*-axis. Three-layer perovskite slabs composed of inner layers of $[\text{XeO}_6]^{4-}$ (peroxenate) octahedra (yellow), which are sandwiched between the layers of neutral XeO_3 molecules. The latter are linked to the inner layers via supramolecular $\text{Xe}\cdots\text{O}$ aerogen bonds that results in the appearance of severely distorted $[\text{O}_3\cdots\text{XeO}_3]$ octahedra (orange–brown). (b, c) Fragments of perovskite-type slab in skeletal and polyhedral representations, which illustrate aerogen interactions between the $[\text{XeO}_6]^{4-}$ octahedra and $[\text{XeO}_3]^0$ molecules. Positions of BCPs are indicated with green balls. Xe–O distances are given in Å. Thermal displacement ellipsoids are shown at the 30% probability level. Potassium ions have been omitted for clarity.

Table 1. Comparison of Xenon–Oxygen Bond Properties of $\text{K}_4\text{Xe}_3\text{O}_{12}$ and XeO_3

bond	distance (Å)	ρ_b ($\text{e} \text{\AA}^{-3}$) ^a	$\nabla^2(\rho)$ ($\text{e} \text{\AA}^{-5}$) ^b	H_b (a.u.) ^c	ϵ^d	note
$\text{K}_4\text{Xe}_3\text{O}_{12}$						
$\text{Xe}(1)\cdots\text{O}(1)$	$2.475(9) \times 3$	0.3112	+3.4107	-0.0032	0.0331	aerogen bonds ^e
$\text{Xe}(1)\cdots\text{O}(2)$	$1.774(7) \times 3$	1.3814	+8.4690	-0.1439	0.0125	covalent bonds in $[\text{XeO}_3]^0$ molecule
$\text{Xe}(2)\cdots\text{O}(1)$	$1.821(9) \times 6$	1.2901	+6.3218	-0.1302	0.0006	covalent bonds in $[\text{XeO}_6]^{4-}$ octahedron ^f
XeO_3^g						
$\text{Xe}(1)\cdots\text{O}(1)$	1.74(3)	1.4655	+10.9628	-0.1584	0.0109	covalent bond at $\text{Xe}(1)\cdots\text{O}(1)\cdots\text{Xe}(1)$ bridge
$\text{Xe}(1)\cdots\text{O}(1)$	2.80(3)	0.1561	+2.0215	+0.0019	0.0607	aerogen bond at $\text{Xe}(1)\cdots\text{O}(1)\cdots\text{Xe}(1)$ bridge
$\text{Xe}(1)\cdots\text{O}(2)$	1.76(3)	1.4066	+8.9539	-0.1477	0.0130	covalent bond to nonbridging oxygen
$\text{Xe}(1)\cdots\text{O}(3)$	1.77(3)	1.3987	+8.4175	-0.1479	0.0103	covalent bond at $\text{Xe}(1)\cdots\text{O}(3)\cdots\text{Xe}(1)$ bridge
$\text{Xe}(1)\cdots\text{O}(3)$	$2.90(3) \times 2$	0.1260	+1.6600	+0.0021	0.0715	aerogen bonds at $\text{Xe}(1)\cdots\text{O}(3)\cdots\text{Xe}(1)$ bridges

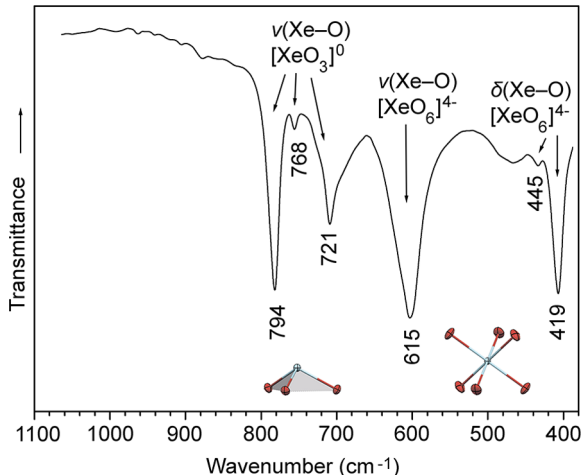
^aElectron density at the BCP. ^bLaplacian of electron density at the BCP. ^cTotal electronic energy density at the BCP. ^dBond ellipticity. ^eAngles at $\text{Xe}(1): \text{O}(1)-\text{Xe}(1)-\text{O}(1) = 85.3(3)^\circ \times 3; \text{O}(2)-\text{Xe}(1)-\text{O}(2) = 100.3(3)^\circ \times 3$. ^fAngles $\text{O}(1)-\text{Xe}(2)-\text{O}(1)$ are $90.9(4) \times 3$ and $89.1(4) \times 3$.

^gBond properties of XeO_3 were calculated on the basis of structural data reported by Templeton et al.¹⁸

Laplacian operator¹⁹ is indicative of a closed shell (non-covalent) character of aerogen interactions, whereas nearly zero values of the total electronic energy density of Cremer and Kraka (H_b) corroborate with weakness of aerogen bonding.²⁰ The relative high values of aerogen bond ellipticities suggest for high degree of electron delocalization.¹⁹ Aerogen bonding belongs to a family of weak σ -hole interactions defined by the occurrence of region of positive molecular electrostatic potential (σ -hole).¹⁷ It is worth noting that although computation of electrostatic potential distribution is an ordinary task for molecular systems, it is still a challenge in case of three-dimensional inorganic frameworks containing heavy elements.²¹ In this respect, we suggest that the set of

bond properties listed in Table 1 can alternatively define the occurrence of aerogen interactions in xenon compounds.

The properties of covalent bonds in $[\text{XeO}_3]^0$ structural units are very similar to both $\text{K}_4\text{Xe}_3\text{O}_{12}$ and XeO_3 (Table 1), whereas aerogen bonds in $\text{K}_4\text{Xe}_3\text{O}_{12}$ are noticeably shorter (and stronger) than corresponding linkages in XeO_3 . Because the oxygen atoms involved in aerogen bonding play a role of bridges between aerogen and covalent linkages (Figure 2, Table 1), one could expect that strengthening of aerogen bonds in $\text{K}_4\text{Xe}_3\text{O}_{12}$ relative to XeO_3 would affect the frequencies of Xe–O vibrations in IR spectra. That suggestion is consistent with the experimental data: peak positions of IR absorption bands of $\text{K}_4\text{Xe}_3\text{O}_{12}$ (Figure 3, Table 2) are blue-shifted (toward small

Figure 3. IR spectrum of $\text{K}_4\text{Xe}_3\text{O}_{12}$.Table 2. Vibrational Assignments for Infrared Absorption Bands (cm^{-1}) of $\text{K}_4\text{Xe}_3\text{O}_{12}$ (1), $\text{KBa}(\text{XeNaO}_6)$ (2), and XeO_3 (3)

1 ^a	2 ^b	3 ^c	assignment ^d
794 (795)		820	$\nu(\text{Xe–O})$ of $[\text{XeO}_3]^0$
768 (788)		— ^e	$\alpha\nu(\text{Xe–O})$ of $[\text{XeO}_3]^0$
721 (700) ^f		780	single $\nu(\text{Xe–O})$ of $[\text{XeO}_3]^0$
615 (612)	690		$\nu(\text{Xe–O})$ of $[\text{XeO}_6]^{4-}$
445 (— ^e)			$\delta(\text{Xe–O})$ of $[\text{XeO}_6]^{4-}$
419 (405)	405	452	$\delta(\text{Xe–O})$ of $[\text{XeO}_6]^{4-}$

^aThis work, suspension in paraffin oil. Data in parentheses: Spittler et al. (1966), AgCl matrix.¹⁸ ^bRef 3. ^cRef 18. ^d ν , symmetric stretching mode; $\alpha\nu$, antisymmetric stretching mode. Assignments were made based on comparison with computational results and IR spectra of perxenate compounds. Bending modes of neat XeO_3 lie in the range of 350 – 320 cm^{-1} .¹⁸ ^eThis band is visible on the given IR spectrum but not mentioned in the text of the reference.¹⁸ ^fOverlapped with the absorption band of paraffin oil (722 cm^{-1}), which could not be completely eliminated by background subtraction.

wavenumbers) relative to corresponding vibrations of XeO_3 and $\text{KBa}(\text{XeNaO}_6)$ (the structure of the latter contains perfect $[\text{XeO}_6]^{4-}$ octahedra).^{3,18} The blue shift effect is well established phenomenon in vibrational spectroscopy of hydrogen bonding²² but a novel one among xenon compounds.

$\text{K}_4\text{Xe}_3\text{O}_{12}$ is the first example of a compound where aerogen bonds maintain the integrity of rigid structural units, that is, perovskite-type slabs in the layered perovskite structure. Because the literature related to this novel type of interactions is still restricted to computational modeling of molecular systems²³ and in view of recent progress in studies of bonding motifs of noble gas compounds,²⁴ the experimental evidence reported herein might provide more insight into the nature of this intricate type of bonding.

The occurrence of aerogen bonds in $\text{K}_4\text{Xe}_3\text{O}_{12}$ and XeO_3 might be a reason for explosive properties and high shock sensitivity of both oxides.^{4,18} It is known that detonation response in high-energetic compounds is often accounted for the breaking of weak interactions playing the role of “trigger bonds”.²⁵ It is likely that weak $\text{Xe(VI)}\cdots\text{O}$ aerogen interactions are those trigger bonds in $\text{K}_4\text{Xe}_3\text{O}_{12}$ (and XeO_3 , respectively) because neither known oxygen- nor halogen-bearing²⁶ layered perovskites possess explosive properties.

The existence of $\text{K}_4\text{Xe}_3\text{O}_{12}$ as well as recently reported xenon perovskites $\text{KM}(\text{XeNaO}_6)$ ($\text{M} = \text{Ca}, \text{Sr}, \text{Ba}$)³ is evidence for the ability of high-valence xenon to replicate polycondensed 2D- and 3D- oxide architectures typical for transition metals such as Ti, Nb, and Ta. This opens up new perspectives for the construction of Xe-based counterparts of titanates, niobates, tantalates, and polyoxometalates by taking into account the charge-balance restrictions imposed by the high oxidation state of octavalent xenon.

ASSOCIATED CONTENT

S Supporting Information

The Supporting Information is available free of charge on the ACS Publications website at DOI: 10.1021/jacs.6b09056.

Synthesis and characterization of $\text{K}_4\text{Xe}_3\text{O}_{12}$; crystallographic data collection details and refinement summary; X-ray powder diffraction data; computational details (PDF)

Crystallographic data (CIF)

AUTHOR INFORMATION

Corresponding Author

*sergei.britvin@spbu.ru

Notes

The authors declare no competing financial interest.

ACKNOWLEDGMENTS

This research was supported by St.-Petersburg State University Grant No. 3.37.222.2015. The authors thank the X-ray Diffraction Center, Computer Resource Center, Geomodel Center, and Center for Optical and Laser Materials Research of St.-Petersburg State University for instrumental support.

REFERENCES

- (a) Bartik, K.; Luhmer, M.; Dutasta, J.-P.; Collet, A.; Reisse, J. *J. Am. Chem. Soc.* **1998**, *120*, 784–791. (b) Gerken, M.; Schrobilgen, G. *J. Coord. Chem. Rev.* **2000**, *197*, 335–395. (c) Frohn, H.-J.; Bardin, V. V. *Organometallics* **2001**, *20*, 4750–4762. (d) Seppelt, K. Z. *Anorg. Allg. Chem.* **2003**, *629*, 2427–2430. (e) Bagno, A.; Saielli, G. *Chem. - Eur. J.* **2003**, *9*, 1486–1495. (f) Fogarty, H. A.; Berthault, P.; Brotin, T.; Huber, G.; Desvaux, H.; Dutasta, J.-P. *J. Am. Chem. Soc.* **2007**, *129*, 10332–10333. (g) Brock, D. S.; Schrobilgen, G. J. *J. Am. Chem. Soc.* **2011**, *133*, 6265–6269. (h) Brock, D. S.; Schrobilgen, G. J.; Žemva, B. *Comprehensive Inorganic Chemistry II*; Reedijk, J., Poeppelmeier, K., Eds.; Elsevier, 2013; Vol. 1, pp 755–822. (i) Nabiev, S. S.; Sokolov, V. B.; Chaivanov, B. B. *Russ. Chem. Rev.* **2014**, *83*, 1135–1180. (j) Rouskala, J.; Zhu, J.; Giri, C.; Rissanen, K.; Lantto, P.; Telkkii, V.-V. *J. Am. Chem. Soc.* **2015**, *137*, 2464–2467. (k) Haner, J.; Schrobilgen, G. J. *J. Chem. Rev.* **2015**, *115*, 1255–1295. (l) Ivanova, M. V.; Mercier, H. P. A.; Schrobilgen, G. J. *J. Am. Chem. Soc.* **2015**, *137*, 13398–13413. (m) Dewaele, A.; Worth, N.; Pickard, C. J.; Needs, R. J.; Pascarelli, S.; Mathon, O.; Mezouar, M.; Irfune, T. *Nat. Chem.* **2016**, *8*, 784–790.
- (a) Gerken, M.; Schrobilgen, G. J. *Inorg. Chem.* **2002**, *41*, 198–204. (b) Forgeron, M. A. M.; Wasylshen, R. E.; Gerken, M.; Schrobilgen, G. J. *Inorg. Chem.* **2007**, *46*, 3585–3592. (c) Vent-Schmidt, T.; Goettel, J. T.; Schrobilgen, G. J.; Riedel, S. *Chem. - Eur. J.* **2015**, *21*, 11244–11252.
- (3) Britvin, S. N.; Kashtanov, S. A.; Krzhizhanovskaya, M. G.; Gurinov, A. A.; Glumov, O. V.; Strekopytov, S.; Kretser, Yu. L.; Zaitsev, A. N.; Chukanov, N. V.; Krivovichev, S. V. *Angew. Chem., Int. Ed.* **2015**, *54*, 14340–14344.
- (4) (a) Appelman, E. H.; Malm, J. G. *J. Am. Chem. Soc.* **1964**, *86*, 2141–2148. (b) Koch, C. W.; Williamson, S. M. *J. Am. Chem. Soc.*

- 1964, 86, 5439–5444. (c) Spittler, T. M.; Jaselskis, B. *J. Am. Chem. Soc.* 1966, 88, 2942–2943.
- (5) The identity with the previously reported substance⁴ has been confirmed by semiquantitative X-ray fluorescence analysis (K and Xe), IR spectrum, X-ray powder diffraction pattern, and structural analysis. Structure solution and refinement were carried out using *SHELXL-2014* and *Olex2-1.2* software.⁶ Extended details are provided in the Supporting Information.
- (6) (a) Sheldrick, G. M. *Acta Crystallogr., Sect. C: Struct. Chem.* 2015, 71, 3–8. (b) Dolomanov, O. V.; Bourhis, L. J.; Gildea, R. J.; Howard, J. A. K.; Puschmann, H. *J. Appl. Crystallogr.* 2009, 42, 339–341.
- (7) Mitchell, R. H. *Pervoskites Modern and Ancient*; Almaz Press: Thunder Bay, Ontario, 2002.
- (8) (a) Fedorov, N. F.; Mel'nikova, O. V.; Saltykova, V. A.; Chistyakova, M. V. *Zh. Neorg. Khim.* 1979, 24, 1166–1170. (b) Konstantinov, P.; Krezhov, K.; Svab, E.; Meszaros, G.; Tork, G. *Phys. B* 2000, 276–278, 260–261.
- (9) (a) Shimoda, Y.; Doi, Y.; Hinatsu, Y.; Ohoyama, K. *Chem. Mater.* 2008, 20, 4512–4518. (b) Rawal, R.; McQueen, A. J.; Gillie, L. J.; Hyatt, N. C.; McCabe, E. E.; Samara, K.; Alford, N. M.; Feteira, A.; Reaney, I. M.; Sinclair, D. C. *Appl. Phys. Lett.* 2009, 94, 192904. (c) Bezjak, J.; Jančar, B.; Boullay, P.; Rečník, A.; Suvorov, D. *J. Am. Ceram. Soc.* 2009, 92, 3022–3032. (d) Tabacaru, C.; Aguadero, A.; Sanz, J.; Chinelatto, A. L.; Thursfield, A.; Pérez-Coll, D.; Metcalfe, I. S.; Fernandez-Díaz, M. T.; Mather, G. C. *Solid State Ionics* 2013, 253, 239–246. (e) Chinelatto, A. L.; Boulahya, K.; Pérez-Coll, D.; Amador, U.; Tabacaru, C.; Nicholls, S.; Hoelzel, M.; Sinclair, D. C.; Mather, G. *C. Dalton Trans.* 2015, 44, 7643–7653.
- (10) (a) Pauling, L. *The Nature of the Chemical Bond*; Cornell University Press: Ithaca, NY, 1960. (b) Bondi, A. *J. Phys. Chem.* 1964, 68, 441–451. (c) Vogt, J.; Alvarez, S. *Inorg. Chem.* 2014, 53, 9260–9266.
- (11) (a) Bader, R. F. W. *Atoms in Molecules. A Quantum Theory*; Oxford University Press: Oxford, U.K., 1990. (b) Bader, R. F. W. *Chem. Rev.* 1991, 91, 893–928. (c) Bader, R. F. W. *J. Phys. Chem. A* 1998, 102, 7314–7323.
- (12) The CRYSTAL14 software package was used to perform the solid-state DFT calculations.¹³ The Peintinger–Oliveira–Bredow split-valence triple-ζ (pob-TZVP) basis sets¹⁴ were used for K and O, whereas basis set for Xe was taken from the TCM CRYSTAL basis set library (<http://www.tcm.phy.cam.ac.uk/~mdt26/crystal.html>), with the hybrid Becke-3–Lee–Yang–Parr (B3LYP) functional.¹⁵ An analysis of theoretical electron density was performed using the program TOPOND14.¹⁶ Assignments of vibrational modes in IR spectra were made in part on the basis of frequency calculations of XeO_3 molecule (for the details see Supporting Information).
- (13) Dovesi, R.; Orlando, R.; Erba, A.; Zicovich-Wilson, C. M.; Civalleri, B.; Casassa, S.; Maschio, L.; Ferrabone, M.; De La Pierre, M.; D'Arco, P.; Noel, Y.; Causa, M.; Rerat, M.; Kirtman, B. *Int. J. Quantum Chem.* 2014, 114, 1287–1317.
- (14) Peintinger, M. F.; Oliveira, D. V.; Bredow, T. *J. Comput. Chem.* 2013, 34, 451–459.
- (15) (a) Becke, A. D. *J. Chem. Phys.* 1993, 98, 5648–5652. (b) Lee, C.; Yang, W.; Parr, R. G. *Phys. Rev. B: Condens. Matter Mater. Phys.* 1988, 37, 785–789.
- (16) Gatti, C.; Casassa, S. *TOPOND14: User's Manual*; CNR-ISTM: Milano, Italy, 2014.
- (17) (a) Bauzá, A.; Frontera, A. *Angew. Chem., Int. Ed.* 2015, 54, 7340–7343. (b) Wang, H.; Wang, W.; Jin, W. *J. Chem. Rev.* 2016, 116, 5072–5104. (c) Kolar, M. H.; Hobza, P. *Chem. Rev.* 2016, 116, 5155–5187.
- (18) Templeton, D. H.; Zalkin, A.; Forrester, J. D.; Williamson, S. M. *J. Am. Chem. Soc.* 1963, 85, 817.
- (19) (a) Koritsanszky, T. S.; Coppens, P. *Chem. Rev.* 2001, 101, 1583–1627. (b) Gatti, C. Z. *Kristallogr. - Cryst. Mater.* 2005, 220, 399–457. (c) Merino, G.; Vela, A.; Heine, T. *Chem. Rev.* 2005, 105, 3812–3841. (d) Lo Presti, L. L.; Gatti, C. *Chem. Phys. Lett.* 2009, 476, 308–316.
- (20) (a) Cremer, D.; Kraka, E. *Croat. Acta Chem.* 1984, 57, 1259–1281. (b) Angelina, E. L.; Duarte, D. J. R.; Peruchena, N. M. *J. Mol. Model.* 2013, 19, 2097–2106.
- (21) Casassa, S.; Erba, A.; Baima, J.; Orlando, R. *J. Comput. Chem.* 2015, 36, 1940–1946.
- (22) (a) Qian, W.; Krimm, S. *J. Phys. Chem. A* 2002, 106, 6628–6636. (b) Zhang, L.; Wang, Y.; Xu, Z.; Li, H. *J. Phys. Chem. B* 2009, 113, 5978–5984.
- (23) (a) Bauzá, A.; Frontera, A. *Phys. Chem. Chem. Phys.* 2015, 17, 24748–24753. (b) Miao, J.; Song, B.; Gao, Y. *Chem. - Asian J.* 2015, 10, 2615–2618. (c) Bauzá, A.; Frontera, A. *ChemPhysChem* 2015, 16, 3625–3630. (d) Miao, J.; Song, B.; Gao, Y. *Chem. - Eur. J.* 2016, 22, 2586–2589. (e) Gao, M.; Cheng, J.; Li, W.; Xiao, B.; Li, Q. *Chem. Phys. Lett.* 2016, 651, 50–55. (f) Esrafilii, M. D.; Asadollahi, S.; Vakili, M. *Int. J. Quantum Chem.* 2016, 116, 1254–1260. (g) Esrafilii, M. D.; Mohammadian-Sabet, F.; Solimannejad, M. *Chem. Phys. Lett.* 2016, 659, 196–202.
- (24) Borocci, S.; Giordani, M.; Grandinetti, F. *J. Phys. Chem. A* 2015, 119, 6528–6541.
- (25) (a) Xu, X.-J.; Zhu, W.-H.; Xiao, H.-M. *J. Phys. Chem. B* 2007, 111, 2090–2097. (b) Liu, Y.; Gong, X.; Wang, L.; Wang, G.; Xiao, H. *J. Phys. Chem. A* 2011, 115, 1754–1762. (c) Harper, L. K.; Shoaf, A. L.; Bayse, C. A. *ChemPhysChem* 2015, 16, 3886–3892.
- (26) (a) Dance, J. M.; Kerkouri, N.; Soubeyroux, J. L.; Darriet, J.; Tressaud, A. *Mater. Lett.* 1982, 1, 49–52. (b) Schroeder, M.; Hartwig, S.; Krämer, K. W.; Decurtins, S.; Hillebrecht, H. *Inorg. Chem.* 2012, 51, 8385–8393. (c) Wang, Z.; Jing, Q.; Zhang, M.; Dong, X.; Pan, S.; Yang, Z. *RSC Adv.* 2014, 4, 54194–54198. (d) Kim, S. W.; Zhang, R.; Halasyamani, P. S.; Hayward, M. A. *Inorg. Chem.* 2015, 54, 6647–6652.